Surf-riding failure mode: from IMO criterion to Direct Assessment procedure and application on Systematic Series D

Maria Acanfora, *University of Naples Federico II,* maria.acanfora@unina.it
Ermina Begovic, *University of Naples Federico II,* begovic@unina.it
Barbara Rinauro, *University of Naples Federico II,* barbara.rinauro@unina.it

ABSTRACT

The paper follows contemporary development of the second generation IMO intact stability criteria and describes application of vulnerability criteria for surf-riding / broaching to Systematic Series D parent hull. Model D1 is a semi-displacement twin-screw round-bilge hull by Kracht and Jacobsen (1992) representative of several naval ships built during 90ties. The modern hull form and the complete set of resistance and self-propulsion results available for the Systematic Series D models offer a possible benchmark case to support scientific community for further criteria verification.

More in particular, the Direct Assessment of surf-riding failure mode has been addressed by two approaches. The first one is based on the 1 DoF nonlinear differential equation for surge motion solved analytically and the occurrence of homoclinic bifurcation is examined.

The second approach is based on a 6DoF ship dynamics simulation taking into account wave, propeller and maneuvering forces and moments. Instantaneous wetted surface is considered for restoring and Froude-Krylov forces while ship resistance, thrust and maneuvering are based on the calm water performances.

Calculations are performed for four ship speeds at the wave with $\lambda/L = 1$ for different wave steepness. A condition where the occurrence of the surf-riding by 1DoF has been verified, is further analyzed by 6DoF, exploring the effect of the nonlinearity in the Froude Krylov force. The limit wave steepness is found for each considered ship speed.

Keywords: *Surf-riding, IMO SGISC, Direct Assessment, Systematic Series D, Bifurcation analysis, 6DoF ship dynamics*

1. INTRODUCTION

The second generation intact stability criteria (SGISC) are developing since 2002 and now are close to their final approval. This new generation of criteria is structured as a multi-level approach; when vulnerability is detected the next level is performed.

Surf-riding/broaching criteria is one of the failure modes SGISC IMO deals with. Level 1 and Level 2 vulnerability criteria are defined by IMO and are based on surf-riding 2nd threshold, while the Direct Assessment procedure is still in development.

This paper focuses on the vulnerability of surf-riding criteria applied on the Systematic Series D parent hull D1. Level 1 and Level 2 following IMO have been verified previously. A further analysis of the surf-riding phenomena, towards the direct assessment, is described and perfomed comparing two different approaches: one based on the 1DoF nonlinear surge equation, the second is based on a 6DoF time domain simulation of ship dynamics in wave.

In particular, the 1DoF equation of surge motion is solved analytically to find the manifolds of surf riding occurrence. The 6DoF time domain model, which combines seakeeping and maneuvering motions of the ship, allows simulating surf-riding phenomenon up to broaching-to instability.

The comparison of the results obtained by the application of the two different methods is performed for several speeds and steepness.

2. IMO SURF-RIDING CRITERION

Level 1 and Level 2 calculation procedures for surf-riding criteria are defined in IMO documents SDC 2 WP 4 and SDC 3 WP 5.

Umeda (1990) studied the surf riding probability as the “probability for ship to meet peak to peak wave whose height and length are satisfied for the condition for the surf riding in regular waves”. Based on this approach, IMO defines Level 1 vulnerability as limit values of Froude number (Fn>0.3) or ship length (L<200 m).

Spyrou (2006) derived the close form of the Melnikov method for asymmetric surging and surf-riding in extreme following seas, inspired by work of Kan (1990). The main outcome of this work combined with the probability of wave occurrence as previously shown by Umeda (1990), is currently used as IMO SGISC procedure of surf-riding and broaching failure mode.

Level 2 vulnerability is detected if the value of Index *C* is greater than limit value of 0.005.

3. 1 DoF MODEL OF SURGE MOTION EQUATION

The mathematical model for 1 DoF describing surge motion equation is derived from Newton second law:

$$(m + m_X)\dot{u} + R(u) - T(u,n) = F_X \quad (1)$$

m is the ship displacement, m_X is the added mass, and u is the ship speed.

R is the calm water resistance approximated with a 5th order polynomial equation.

$$R = r_0 + r_1 u + r_2 u^2 + r_3 u^3 + r_4 u^4 + r_5 u^5 \quad (2)$$

T is the thrust delivered by the propulsor, expressed by:

$$T = N_P(\tau_0 n^2 + \tau_1 n u + \tau_1 u^2) \quad (3)$$

F_X is the wave excitation calculated considering only the Froude Krylov component f_X in calm water determined with the strip theory method (Belenky 2007, IMO SCD 3 WP.5):

$$F_X = f_X \sin(\omega_e t - kx)$$

$$f_X = \rho g k \zeta_A \sqrt{Fc_i^2 + Fs_i^2} \quad (4)$$

For Surf-riding equilibrium the encounter frequency ω_e is equal to zero therefore the time dependence is neglected.

Defining x_G the distance between center of gravity of the ship and wave trough, equation (1) can be expressed as function wave celerity, c, and ship and wave relative speed in relationship:

$$\dot{x}_G = u - c$$

$$\ddot{x}_G = \frac{1}{(m+m_X)}\left[T_C - R_C - (A_1\dot{x}_G + A_2\dot{x}_G^2 + A_3\dot{x}_G^3 + A_4\dot{x}_G^4 + A_5\dot{x}_G^5\right] \quad (5)$$

Where:

$$A_1 = r_1 + 2(r_2 - N_P\tau_2)c + 3r_3c^2 + 4r_4c^3 + 5r_5c^4 - N_P\tau_1 n$$
$$A_2 = r_2 + 3r_3c + 6r_4c^2 + 10r_5c^3 - N_P\tau_2$$
$$A_3 = r_3 + 4r_4c + 10r_5c^2$$
$$A_3 = r_4 + 5r_5c \quad (6)$$
$$A_5 = r_5$$
$$T_C = N_P(\tau_0 n^2 + \tau_1 nc + \tau_2 c^2)$$
$$R_C = r_0 + r_1c + r_2c^2 + r_3c^3 + r_4c^4 + r_5c^5$$

This second order nonlinear differential equation has been transformed in a first order system with Runge-Kutta method, and then studied numerically analyzing the stability of the possible fixed points, by the definition of Jacobian matrix, its trace and the determinant.

Furthermore, the surge motion equation has been numerically solved in time domain simulations. The results have been plotted in phase plan diagrams and approximated trajectories of the stable and unstable manifold have been defined in order to represent the first and second threshold of surf-riding phenomena.

4. NUMERICAL SIMULATION 6 DOF MODEL

The numerical model has been developed for the dynamics in waves of the displacement ship. It combines seakeeping and manoeuvring motions. The ship is considered as a rigid intact body.

The main coordinate systems used for describing ship motion are presented in Figure 1, i.e. the inertial system fixed to Earth, with the *X-Y* plane coincident with the still water level, and the body-fixed reference frame having its origin at ship centre of gravity.

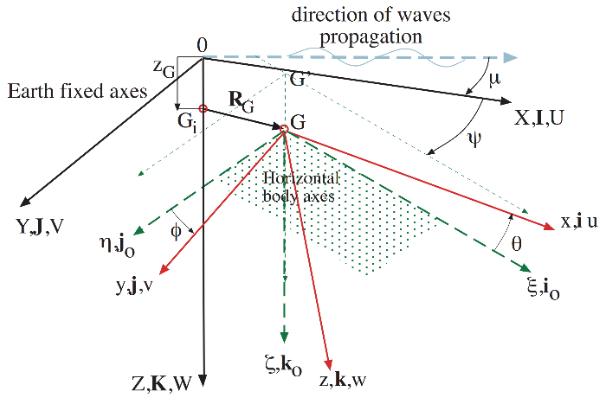

Figure 1: Co-ordinate systems used in ship dynamics (Matusiak 2013).

The hull surface is discretized by means of triangular panels. For each panel, the surface and the normal vector are known. In Eq. 7 the regular wave is calculated in the control points of the hull surface X_c and Y_c (referring to the center of each panel), given in the Earth fixed co-ordinate system by means of a transformation matrix. The coordinates X_c and Y_c take into account the ship's position in waves.

$$\zeta(t) = A\cos[k(X_c cos\beta - Y_c sin\beta) - \omega t] \quad (7)$$

It is important to underline that ω in Eq. 7 is the wave frequency since the longitudinal coordinate X_c depends on ship forward speed. The angle β is the wave heading.

The non-linear 6DoF model is based on the equations of motions in Eq.8. The numerical model can be defined as hybrid or blended (i.e. non-linearities are accounted for restoring and Froude-Krylov actions, while radiation and diffraction actions are obtained by linear strip-theory potential method), and it is based on the assumptions explained in (Matusiak 2013).

$$(m + a_{11})\dot{u} + m(qw - rv) + a_{15}\dot{q} = -mgsin\theta + X_{wave} + X_{man} - b_{15}q + X_{prop} + X_{resist}$$

$$(m + a_{22})\dot{v} + m(ru - pw) + a_{24}\dot{p} + a_{26}\dot{r} = mgcos\theta sin\phi + Y_{wave} + Y_{man} - b_{22}v - b_{24}p$$

$$(m + a_{33})\dot{w} + m(pv - qu) + a_{35}\dot{q} = mgcos\theta cos\phi + Z_{wave} - b_{33}w - b_{35}q$$

$$(I_x + a_{44})\dot{p} + (I_z - I_y)qr + a_{42}\dot{v} + a_{46}\dot{r} = K_{wave} + K_{man} - b_{44}p - b_{42}v - b_{46}r$$

$$(I_y + a_{55})\dot{q} + (I_x - I_z)rp + a_{15}\dot{u} + a_{53}\dot{w} = M_{wave} - B_{55}q - b_{53}w - b_{51}u$$

$$(I_z + a_{66})\dot{r} + (I_y - I_x)pq + a_{62}\dot{v} + a_{64}\dot{p} = N_{wave} + N_{man} - b_{66}r - b_{64}p \quad (8)$$

The terms a_{ij} and b_{ij} are respectively the added mass and damping coefficients at the encounter wave frequency. The terms with the subscript *"wave"* include Froude-Krylov, diffraction and restoring forces and moments, while the terms with the subscript *"man"* refer to manoeuvring actions (i.e. further forces acting in the transversal direction and not included in the hull-wave interaction). The term X_{prop} and X_{resist} models ship propeller actions and hull resistance, respectively, at a given speed.

The inertia, Froude-Krylov and restoring forces and moments are evaluated accounting for all the pertinent non-linearities. The pressure profile is assumed by applying the so called "stretched distribution" above the waterline:

$$p = g\zeta e^{-k(Z_c+\zeta)} + Z_c \quad (9)$$

Where ζ is the wave profile, k is the wave number and Z_c is the depth of any panel, accounting for the actual ship motions.

This approach is a kind of extension of the linear wave theory to incorporate the nonlinear effects associated with the variation of a ship's wetted surface in the Froude-Krylov and hydrostatics forces and moments. Damping, added mass and diffraction forces and moments are calculated beforehand by a potential strip theory code (Faltinsen 1990 and Salvesen et al. 1970) and then implemented in the numerical model.

The numerical model accounts for ship velocity given by the propeller behavior, together with ship resistance in waves. Propeller actions are expressed in body fixed reference frame and move with the hull (see Fig.1).

The total thrust provided by the propellers is evaluated from a known open water characteristic of the propeller, $K_T = K_T(J)$, as follows:

$$X_{prop} = N_P \rho n^2 D^4 K_T \quad (10)$$

where J is the advance ratio, N_P is the number of the propellers, n is the propeller revolutions per second and D is the propeller diameter.

The required propeller revolution n, for still water and constant forward speed, is set in order to obtain the condition:

$$X_{prop} = X_{resist}$$

where:

$$X_{resist} = \frac{R_T}{1-t} = -0.5\rho u^2 S C_T/(1-t) \quad (11)$$

In (11), R_T is the total resistance, t is the thrust deduction factor, S is the static wetted surface and u is the forward velocity of the ship in the body-fixed co-ordinate system.

Propeller revolution is kept constant during the simulations in waves. Therefore, ship speed will modify from still water value, due to added resistance in waves. This is evaluated as a result of dynamic pressures forces, acting on the wetted panel on the ship, projected on x-direction.

Maneuvering actions are estimated by semi-empirical model. The so-called *slow motion hydrodynamic derivatives* for maneuvering motions are evaluated for the still water condition. The argument is that these terms include the effects that are related to slow motion, and they are mainly governed by the non-potential flow effects. This way of modelling ship manoeuvring may be questioned for the ship operating in waves. However, it proved to yield reasonable results. A good compromise is to preserve only the terms related to velocities such as Y_v, Y_r, N_v and N_r without including added mass contribution in the manoeuvring model, as these are already included in the radiation forces model. (Acanfora and Matusiak 2016).

In the current simulations, the potential damping terms related to yaw and sway motions in wave are neglected. Dealing with surf-riding, which involves encounter frequencies close to zero, the above assumption is supported by the evidence that in such condition, potential damping tends to null values.

The linear model for ship maneuvering limits the maneuvering forces only to the linear coefficients (i.e. to the motion derivatives). These can be easily estimated from the semi-empirical formulae obtained by the regression analysis. The linear maneuvering coefficients are given in Eq. 12, where T is the ship draft:

$$Y_v = -\pi(T/L)^2\ [1 + 0.4C_B(B/T)]$$
$$Y_r = -\pi(T/L)^2\ [-0.5 + 2.2(B/L) - 0.08(B/T)]$$
$$N_v = -\pi(T/L)^2\, [0.5 + 2.4(T/L)]$$
$$N_r = -\pi(T/L)^2\ [0.25 + 0.039(B/T) - 0.56(B/L)] \tag{12}$$

The assumptions on maneuvering model do not concern surf-riding developments; indeed they will affect the development of broaching instability.

5. SYSTEMATIC SERIES D OF FAST TWIN SCREW DISPLACEMENT SHIPS

The systematic Series D is originated from a semi-displacement twin-screw round-bilge hull form, initially made by the German yard Howaldtswerke-Deutsche Werft, with the necessity of having resistance and power predictions on a shorter and wider ship as this was a new and developing trend of ship design. (Kracht 1992, Kracht and Jacobsen, 1992).

The D-Systematic Series has seven models, derived from two parent hull forms D1 and D5. Resistance and propulsion tests have been performed in calm water in a speed range of Froude's number from 0.15 to 0.80.

6. IMO LEVEL 1 AND LEVEL 2 CRITERIA RESULS

The body plans of Systematic series D and ship main dimensions scaled to 90 m length are reported in (Begovic et al. 2018, Rinuaro and Begovic. 2019). All seven models result vulnerable to level 1 and level 2 criteria at given ship service speed of Fn = 0.433. Therefore, Froude number limit values, over which surf-riding is likely to occur, have been defined and reported in Begovic et al. (2018). Performing level 2, Froude number limit is around 0.325-0.34, depending on the type of hull, instead of 0.30 defined by the 1st level. With this result, an increase of ship speed of about 1 - 2 knots is obtained without been vulnerable to surf-riding and broaching. It has been shown that in the case of hull forms with the same length and tested with the same propeller, models with the lower calm water resistance resulted less vulnerable to the surf riding occurrence.

7. TOWARDS DIRECT ASSESSMENT

Based on the results found applying IMO criteria, similar for all Systematic Series D models, a further analysis towards direct assessment has been performed for hull D1.

The 1DoF and 6DoF models have been performed for λ/L = 1 wave case and for four Froude number cases. The limit value of steepness, to avoid surf riding, has been defined for each ship speed.

It is important to point out the implicit difference between the two methods: 1Dof model analytically finds the equilibrium points considering the ship speed equal to celerity and identifies stable and unstable manifolds from the unstable equilibrium points by numerical simulation in time to assess surf-riding developments.

On the other hand, 6DoF model simulates the effective speed of the ship in waves caused by the solution of the dynamic problem in time domain. Therefore surf-riding is observed in the simulation if the ship speed at a certain time equals the wave celerity.

1 DoF methodology

The analytical study of the surge motion equation brings to the definition of equilibrium points between the three forces acting on the ship: T_C, R_C and F_X, where T_C, and R_C are calculated for the wave celerity value c equal to 11.85m/s.

Figure 2 shows different equilibrium conditions for $\lambda/L = 1$ and $Fn = 0.335$ ($u = 9.95$m/s) and three different steepness. The input number of revolutions per second n is imposed to reach ship nominal speed; for Fn=0.335, n is equal to 2.9107 rps.

For $H/\lambda = 1/50$ no fixed points are found and the only possible motion is surging. As steepness increases, H/λ = 1/45 and 1/40, surf-riding phenomenon becomes possible, defined by infinite points of equilibrium.

By numerical simulation of the surge motion, the phase plan can be used to study the occurrence of surf-riding. Figure 3 to 6 show the phase plans, with displacement and cosine function of displacement, reporting the trajectories of the manifold that divide the different domains of attractions. Figures 3 and 5 report wave steepness case that generates surf-riding condition between 1st and 2nd threshold (for definition of surf-riding thresholds see Belenky 2011), where the stable manifold (continuous line) defines the only surf-riding domain, while the rest of the plane defines surge motion, and the unstable manifold (dashed line) converge to the stable equilibrium point. Figures 4 and 6 report surf-riding over 2nd threshold. The phase plans with cosine function, given in Figures 5 and 6 show the homoclinic bifurcation occurring for surf-riding 2nd threshold, as reported in Spyrou (1996).

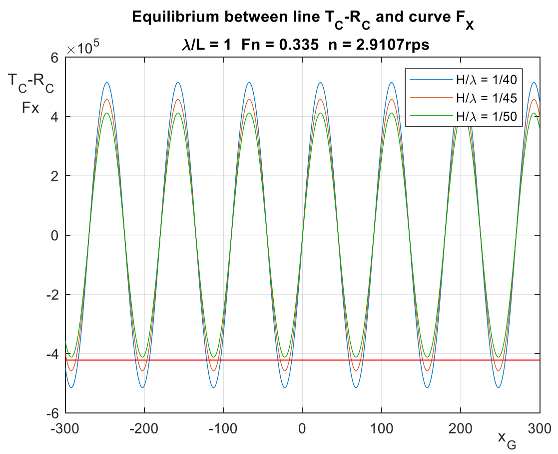

Figure 2: Equilibrium between T_C-R_C and F_X, for λ/L=1, *F*n=0.335 and 3 steepness

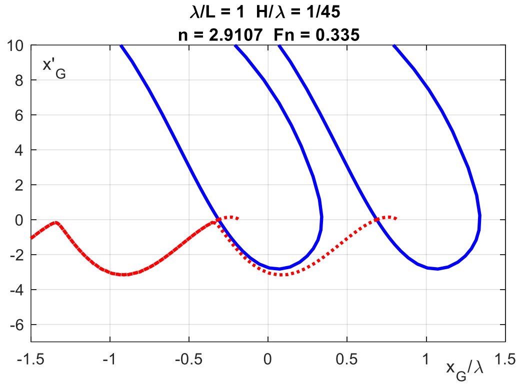

Figure 3: Phase plan for λ/L=1, *F*n=0.335 and H/λ=1/45 - between 1st and 2nd threshold

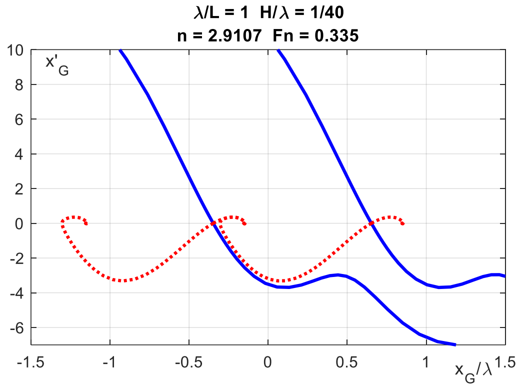

Figure 4: Phase plan for λ/L=1, *F*n=0.335 and H/λ=1/40 – over 2nd threshold

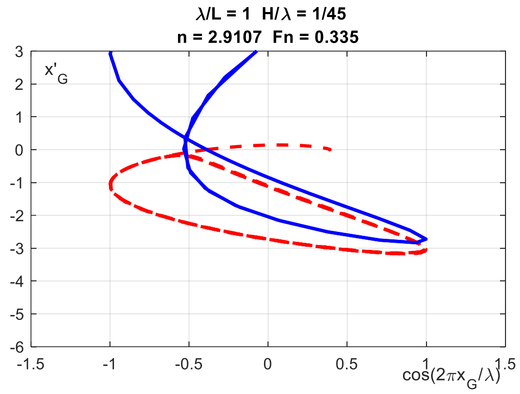

Figure 5: Phase plan with cosine function for λ/L=1, *F*n=0.335 and H/λ=1/45 - between 1st and 2nd threshold

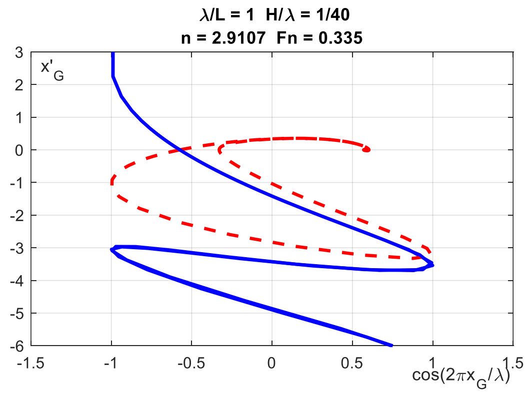

Figure 6: Phase plan with cosine function for λ/L=1, *F*n=0.335 and H/λ=1/40 – over 2nd threshold

6 DoF methodology

Time domain simulations work on a sinusoidal wave, defined by length and steepness, starting with initial Froude number, Fn_{int}, that sets the propeller revolution and the initial encounter frequency (for radiation and diffraction forces).

Calculations have been performed for two cases, based on different pressure integrations for the Froude-Krylov Forces. The first case considers linear Froude-Krylov Forces integrated on the wetted surface coincident with the calm water one; the second case (nonlinear Froude-Krylov) considers the effective wetted surface due to wave elevation and ship dynamics. However, in both cases, restoring forces include the pertinent nonlinearities.

Figures 7 through 9 show time domain simulations for X_{prop}-$X_{Resistance}$ and FK_L (linear Froude Krylov), ship speed u, and yaw angle ψ for wave case $\lambda/L = 1$, $H/\lambda = 1/50$ and $Fn_{int} = 0.35$ corresponding to n=3.0726 rps. This case features the dynamic equilibrium of surging, where all forces oscillate in time.

Increasing the steepness to $H/\lambda = 1/40$ after a certain number of oscillations surf-riding phenomenon can be observed form figures 10 to 12, when X_{prop}-$X_{Resistance}$ and FK_L equilibrate and Fn and yaw angle remain constant. The ship will experience surf-riding until yaw angle increases and generates instability corresponding to broaching phenomena.

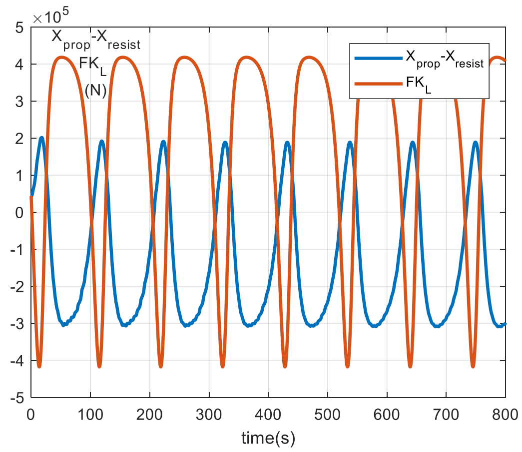

Figure 7: X_{prop}-X_{Resist}, and FK_L time domain simulation for λ/L=1, Fn_{int}=0.35 and H/λ=1/50 , for Linear Froude Krylov case– surging condition

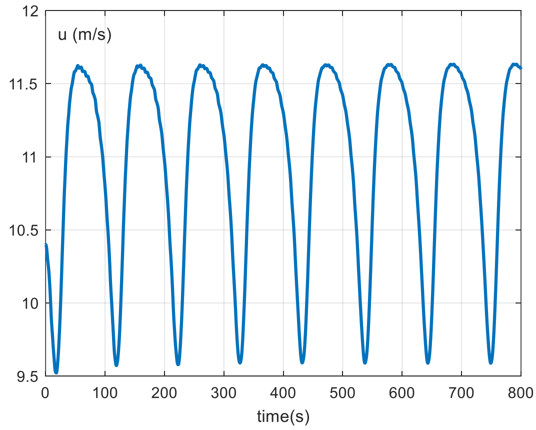

Figure 8: Speed time domain simulation for λ/L=1, Fn_{int}=0.35 and H/λ=1/50, for Linear Froude Krylov case – surging condition

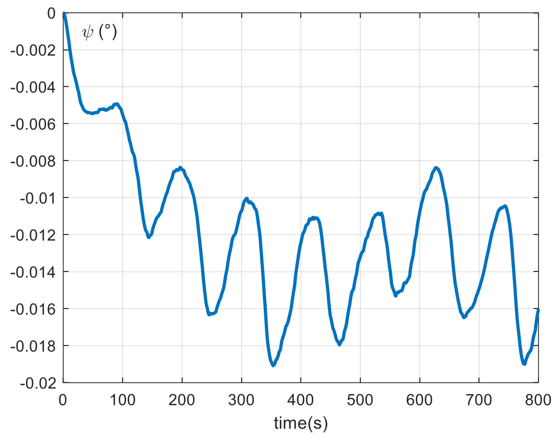

Figure 9 Yaw angle time domain simulation λ/L=1, Fn_{int}=0.35 and H/λ=1/50, for Linear Froude Krylov case – surging condition

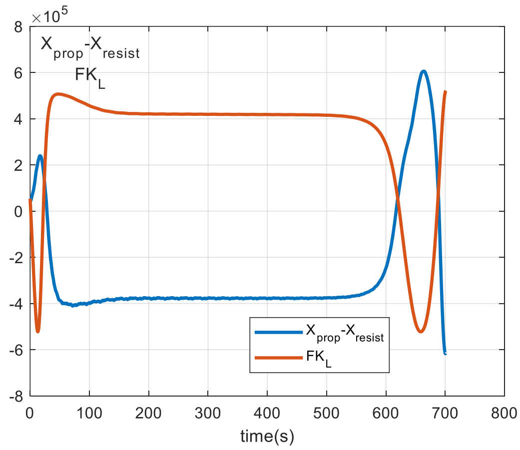

Figure 10: X_{prop}-X_{Resist}, and FK_L time domain simulation for λ/L=1, Fn_{int}=0.35 and H/λ=1/40, for Linear Froude Krylov case – surf-riding/broaching phenomena

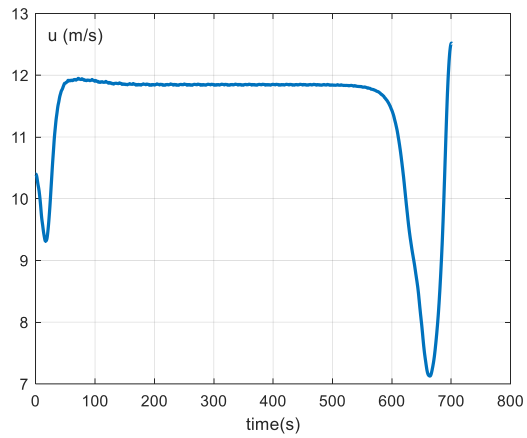

Figure 11: Speed time domain simulation for λ/*L*=1, *F*n$_{int}$=0.35 and *H*/λ=1/40, for Linear Froude Krylov case – surf-riding/broaching phenomena

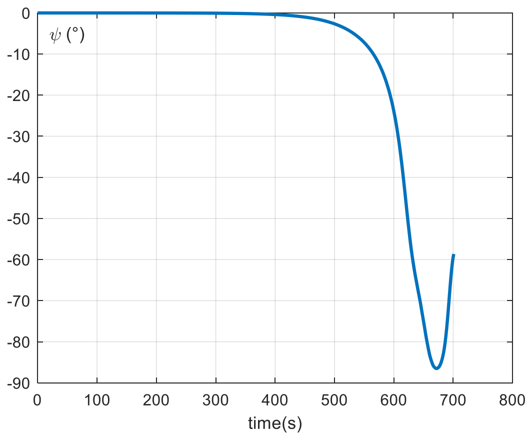

Figure 12: Yaw angle time domain simulation for λ/*L*=1, *F*n$_{int}$=0.35 and *H*/λ=1/40, for Linear Froude Krylov case – surf-riding/broaching phenomena

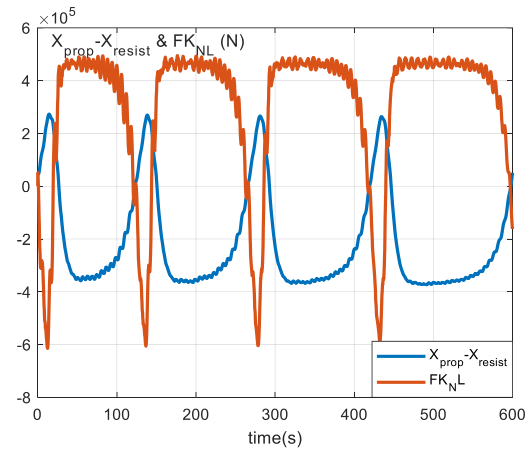

Figure 13: X_{prop}-X_{Resist}, and FK_{NL} time domain simulation for λ/*L*=1, *F*n$_{int}$=0.35 and *H*/λ=1/50 – surging condition

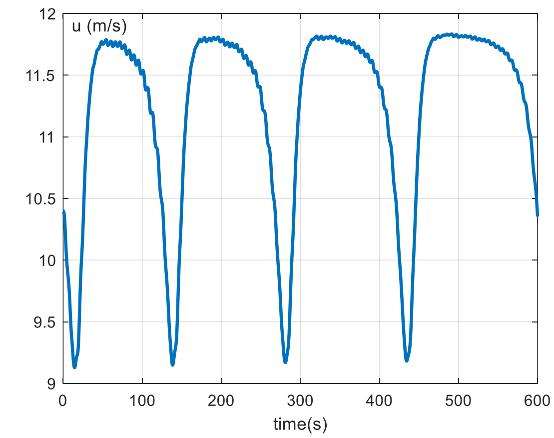

Figure 14: Speed time domain simulation for λ/*L*=1, *F*n$_{int}$=0.35 and *H*/λ=1/40, for Nonlinear Froude Krylov case – surging condition

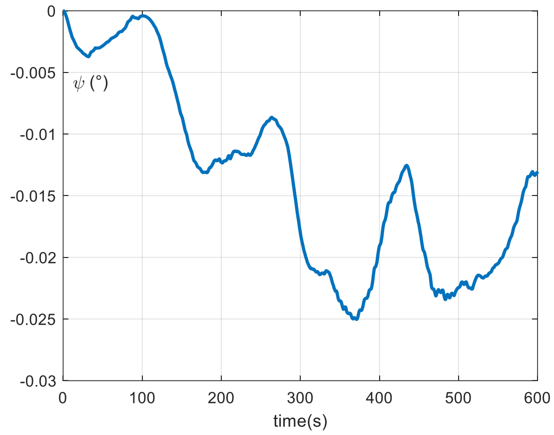

Figure 15 Yaw angle time domain simulation λ/*L*=1, *F*n$_{int}$=0.35 and *H*/λ=1/50, for Nonlinear Froude Krylov case – surging condition

Figures 13 to 15 represent time domain simulations for X_{prop}-$X_{Resistance}$, FK_{NL} (nonlinear Froude Krylov), *F*n, and yaw angle, by nonlinear Froude Krylov forces, for wave case λ/*L* = 1, *H*/λ = 1/40 and *F*n$_{int}$ = 0.35. It can be seen how considering the nonlinearity of Froude Krylov forces, surf-riding is not detected for the same conditions of linear Froude Krylov case.

Comparison of 1 DoF and 6 DoF results

Figure 16 summarizes the main results for four Froude number cases comparing the different approaches discussed above. The ship is identified as vulnerable to surf-riding if the wave steepness exceeds the value above the limit line:

- Blue line, square markers for 6DoF approach with nonlinear Froude-Krylov forces
- Red line, triangle markers for 6DoF approach with linear Froude-Krylov forces
- Grey line, round markers for 1Dof approach

It can be observed that 1 DoF method is more conservative than the 6 DoF ones (both linear and nonlinear Froude Krylov cases). However, for ship speed *u* converging to wave celerity *c*, all methods predict the surf-riding phenomenon at the same steepness, around 0.006. Concerning the 6 DoF approach, all nonlinearities due to instantaneous wetted surface, for small wave amplitudes, are converging to their linear values.

For ship speeds far from the wave celerity, the adopted methods provide distinct threshold values. The 1DoF linear and the 6DoF linear outcomes are closer to each other than 6DoF nonlinear.

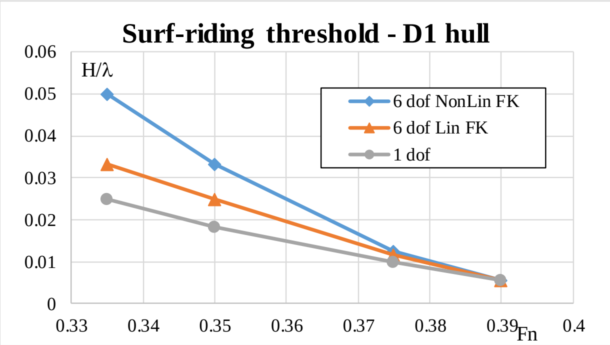

Figure 16: Comparison of 1 DoF and 6 DoF results

8. CONCLUSIONS

The present work explores the possibility of Direct Assessment approaches for surf riding phenomenon by bifurcation analysis of 1 DoF surge motion equation and 6 DoF ship dynamics simulation, considering two cases: linear and nonlinear Froude-Krylov Forces.

The different methodologies have been applied on Systematic Series D parent hull, for four nominal Froude numbers and wave case $\lambda/L=1$ and surf riding thresholds have been defined through wave steepness.

As expected, 1 DoF method is more conservative than the 6 DoF ones. A possible explanation in the different results between 1DoF and 6DoF linear Froude-Krylov model can be attributed to the non-linarites in restoring forces. Moreover, the 6DoF approach with nonlinear Froude-Krylov forces leads to the less conservative thresholds.

Based on the above considerations, a two-fold approach can be envisaged applying 1DoF and 6DoF nonlinear: 1DoF approach, faster and easier to implement, might be used to set the initial steepness value for the 6DoF simulations.

Further step towards direct assessment can be the implementation of resistance and thrust forces calculated in waves by CFD simulations.

REFERENCES

Acanfora, M., and J. Matusiak. 2016. “On the Estimations of Ship Motions during Maneuvering Tasks in Irregular Seas.” In Proceedings of 3rd International Conference on Maritime Technology and Engineering, MARTECH 2016. Vol. 1.

Begovic, E., C. Bertorello, G. Boccadamo, and B. Rinauro. 2018. “Application of Surf-Riding and Broaching Criteria for the Systematic Series D Models.” Ocean Engineering 170 (December). Pergamon: 246–65. https://doi.org/10.1016/J.OCEANENG.2018.08.062.

Belenky V., Bassler C.C., Spyrou K.J., 2011, “Development of second generation intact stability criteria”, Naval surface warfare center Carderock division -50-TR-2011/065, Hydromechanics department report

Belenky V., Sevastianov V., 2007, “Stability and safe of ships, risk of capsizing”, The society of naval architects and marine engineers (SNAME), Jersey City NJ

Dunwoody A.B., 1989, “Roll of a Ship in Astern Seas – Response to GM Fluctuations”, *Journal of Ship Research* 33(4), pp. 284-290.

Faltinsen, O.M. 1990. “Sea Loads on Ships and Offshore Structures”. Cambridge University Press. Vol. 1. https://doi.org/9780521458702.

IMO SDC 3 /WP 5 – Report of the working group (part 1). London, 21 Gen 2016

IMO SDC 2 /WP 4 – Report of the working group (part 1). London, 19 Feb 2015

IMO 2006, “MSC.1/Circ.1200 - Interim Guidelines for Alternative Assessment of the Weather Criterion”, 24 May.

Kan, M. (1990), “A Guideline to Avoid the Dangerous Surf-riding”, Proceedings of the 4th International Conference on Stability of Ships and Ocean Vehicles, University Federico II of Naples (Naples), pp.90-97

Kawahara, Y., Maekawa, K., Ikeda, Y., 2009, “A Simple Prediction Formula of Roll Damping of Conventional Cargo Ships on the Basis of Ikeda’s Method and Its Limitation”, Proceedings of the 10th International Conference on Stability of Ships and Ocean Vehicles, (STAB2009), St. Petersburg, Russia, pp. 387-398.

Kracht A., 1992, internal report – VWS-Bericht Nr. 1202/92

Kracht A. M., Jacobsen A., 1992, “D-series Systematic Experiments with Models of Fats Twin-screw Displacement Ship”, SNAME transactions, Vol. 100, pp. 199-222

Matusiak, Jerzy. 2013. Dynamics of a Rigid Ship. SCIENZE +. Aalto University publication series. https://aaltodoc.aalto.fi/handle/123456789/24408.

Rinauro B., and Begovic E., 2019, "Vulnerability assessment of surf-riding/broaching and pure loss of stability for Systematic Series D1 model", Ships and Offshore Structures, DOI: 10.1080/17445302.2019.1596545

Salvesen N., Tuck E. O., Faltinsen O., 1970, "Ship Motions and sea loads", The society of naval architects and marine engineers

Spyrou K.J., 1996, "Dynamic instability in quartering seas: The behavior of a ship during broaching", Journal of ship research, 40, No 4, 326-336

Umeda, N. (1990), "Probabilistic Study on Surf-riding of a Ship in Irregular Following Seas", Proceedings of the 4th International Conference on Stability of Ships and Ocean Vehicles, University Federico II of Naples (Naples), pp.336-343.